AAPS PharmSciTech, Vol. 14, No. 3, September 2013 (© 2013)
DOI: 10.1208/s12249-013-0008-4

Research Article

Effect of Particle Size on In-die and Out-of-die Compaction Behavior of Ranitidine Hydrochloride Polymorphs

Kailas S. Khomane[1] and Arvind K. Bansal[1,2]

Received 18 April 2013; accepted 5 July 2013; published online 30 July 2013

Abstract. The present study investigates the effect of particle size on compaction behavior of forms I and II of ranitidine hydrochloride. Compaction studies were performed using three particle size ranges [450–600 (A), 300–400 (B), and 150–180 (C) μm] of both the forms, using a fully instrumented rotary tableting machine. Compaction data were analyzed for out-of-die compressibility, tabletability, and compactibility profiles and in-die Heckel and Kawakita analysis. Tabletability of the studied size fractions followed the order; IB > IA > > IIC > IIB > IIA at all the compaction pressures. In both the polymorphs, decrease in particle size improved the tabletability. Form I showed greater tabletability over form II at a given compaction pressure and sized fraction. Compressibility plot and Heckel and Kawakita analysis revealed greater compressibility and deformation behavior of form II over form I at a given compaction pressure and sized fraction. Decrease in particle size increased the compressibility and plastic deformation of both the forms. For a given polymorph, improved tabletability of smaller sized particles was attributed to their increased compressibility. However, IA and IB, despite poor compressibility and deformation, showed increased tabletability over IIA, IIB, and IIC by virtue of their greater compactibility. Microtensile testing also revealed higher nominal fracture strength of form I particles over form II, thus, supporting greater compactibility of form I. Taken as a whole, though particle size exhibited a trend on tabletability of individual forms, better compactibility of form I over form II has an overwhelming impact on tabletability.

KEY WORDS: compaction; Heckel plot; Kawakita analysis; particle size; ranitidine hydrochloride polymorphs.

INTRODUCTION

Tensile strength of pharmaceutical powders has always evoked interest. Tabletability can be used as performance criterion during formulation development and is represented by plot of tablet tensile strength against compaction pressures. Compressibility and compactibility both contribute to tabletability. It has been argued that compressibility is a measure of interparticulate bonding area and compactibility is a measure of interparticulate bonding strength (1–3). Mechanical properties of the material that govern bonding area include plasticity, elasticity, and brittle fragmentation. Moreover, particle size distribution and machine parameters like dwell time also affect the compressibility.

A previous study from our lab investigated the influence of crystal structure on the mechanical properties of ranitidine hydrochloride (RAN) polymorphs (4). It was found that form I, having higher true density, resisted deformation under compaction pressure and exhibited poor compressibility. However, it showed higher tabletability (tensile strength) over form II by virtue of greater compactibility (interparticulate bonding strength). Thus, tabletability of RAN is governed by interparticulate bonding strength. The study concluded that true density, a molecular descriptor of bonding strength (5,6), can be used as a predictor of tabletability.

However, as discussed above, compressibility also contributes to tabletability and particle size has been reported to affect the tabletability of the material by altering the compressibility (7,8). In the previous study, particle size of the both polymorphs was kept similar to establish structure property relationship. Hence, in the present work, the effect of particle size on overall compaction behavior and specifically on tabletability of RAN polymorphs has been investigated. This shall helps in selection of appropriate solid form for pharmaceutical development.

Compaction studies have been performed using different ranges of particle size and compaction pressures, on a fully instrumented rotary tableting machine. Data were analyzed for out-of-die compressibility, tabletability, and compactibility profiles and in-die Heckel and Kawakita analysis. Nominal single particle fracture strength was obtained for the different particle sized fractions of both forms by microtensile testing using texture analyzer.

[1] Department of Pharmaceutics, National Institute of Pharmaceutical Education and Research (NIPER), Sector-67, S. A. S Nagar, Mohali, Punjab, India.
[2] To whom correspondence should be addressed. (e-mail: akbansal@niper.ac.in)

MATERIAL AND METHODS

RAN Polymorphs

Two polymorphs of RAN namely form I and form II were kindly gifted by SMS Pharmaceuticals Ltd., Hyderabad (India).

Powder X-ray Diffraction

Powder X-ray diffraction (PXRD) of as-received samples was recorded at room temperature on Bruker's D8 Advance diffractometer (Bruker AXS, Karlsruhe, Germany) with Cu $K\alpha$ radiation (1.54 Å), at 40 kV, 40 mA passing through nickel filter. Analysis was performed in a continuous mode with a step size of 0.01° and step time of 1 s over an angular range of 3–40° 2θ. Obtained diffractograms were analyzed with DIFFRAC plus EVA, version 9.0 (Bruker AXS, Karlsruhe, Germany) diffraction software.

Differential Scanning Calorimetry

Differential scanning calorimetry (DSC) analysis was performed using DSC, Model Q2000 (TA Instruments, New Castle, DE, USA) operating with Universal Analysis® software, version 4.5A (TA Instruments, New Castle, DE, USA). About 2.5–3.5 mg of RAN was accurately weighed in crimped aluminum pans and subjected to the thermal scan from ambient to 160°C at the heating rate of 1.0°C/min. Dry nitrogen purge was maintained at 50 mL/min. Prior to analysis, instrument was calibrated using high purity standards of zinc (Zn) and indium (In).

Moisture Content

Moisture content of as-received samples (300 mg) was determined in triplicate by Karl Fischer titration (Metrohm 794 Basic Titrino, Herisau, Switzerland). Instrument was calibrated with disodium tartrate dihydrate for the accuracy of moisture determination.

Particle Size Distribution

Four different particle size ranges, 650–800, 450–600, 300–400, and 150–180 μm, were obtained by sieving from the bulk material. D_{90} and D_{50} of each fraction were determined by optical microscopy by measuring diameter along the longest axis, for at least 200 particles (DMLP microscope, Leica Microsystems, Wetzlar, Germany). Compaction behavior of the largest particle size fraction, i.e., 650–800 μm, could not be performed as required amount of sample could not be obtained through bulk sieving.

Scanning Electron Microscopy

Scanning electron microscopy analysis of bulk solids was carried out to study the particle morphology of both the polymorphs using a scanning electron microscope (S-3400, Hitachi Ltd., Tokyo, Japan) operated at an excitation voltage of 15 kV. Powders were mounted onto steel stage using double-sided adhesive tape and coated with gold using ion sputter (E-1010, Hitachi Ltd., Japan).

True Density and Flow Properties

The true density of both the polymorphs was determined in triplicate by helium pycnometry (Pycno 30, Smart Instruments, Mumbai, India) at 25±2°C/30±5% RH.

Bulk density was determined in triplicate by adding accurately weighed (about 100 g) powder to 250 mL graduated measuring cylinder. Corresponding volume was measured to obtain the bulk density. Tapped density was determined, as per USP II method, using Tap density apparatus (Electrolab, Mumbai, India). Flowability of the material was determined by calculating Carr's index.

Single Particle Fracture Strength

The measurement of single particle nominal fracture strength of both the polymorphs was performed using a texture analyzer (TA-XT2i, Stable Micro Systems, Surrey, UK). Instrument was calibrated for both the distance and the load cell. All experiments were performed using 5 kg load cell and 2 mm flat-faced probe. The force–displacement and force–time measurements were obtained by employing a pretest speed of 0.4 mm/s, test speed of 0.2 mm/s (fracture speed), and post-test speed of 0.6 mm/s. The data acquisition rate was 200 points per second using a fully integrated data acquisition and analysis software (Texture Expert, version 1.22, TA-XT2i, Stable Micro Systems, Surrey, UK). A stainless steel support was kept on the platform to support the test particle. The probe was vertically moved down on single particle until it fractured. Fracture strength of 25 single particles from each particle sized fraction was measured at 25±2°C/30±5% RH. The single particle nominal fracture strength of smallest sized fraction (150–180 μm) was not performed, as particle size was too small to carry out the measurement precisely.

Tableting and Data Acquisition

Rotary tablet press (Mini II, Rimek, Ahmedabad, India) was equipped at one of the eight stations with 8 mm D-tooling with flat punch tip. Feed frame was used for uniform die filling and blind dies were used at all other positions. Precompression rollers were set out of function. Powders of each fraction were compacted at a constant volume. Humidity (30±5% RH) and temperature (25±2°C) conditions were monitored throughout the study. Each sized fraction was compacted at different compaction pressures on an instrumented rotary tablet press ranging from around 0 to 400 MPa. The tableting speed was kept constant at 14.0 rpm.

Data were acquired by Portable Press Analyzer™ (PPA) version 1.2, revision D (Data Acquisition and Analyzing System, PuuMan Oy, Kuopio, Finland), through an infrared (IR) telemetric device with 16-bit analog-to-digital converter (6 kHz). Force was measured by strain gauges at upper and lower punches (350×, full Wheatstone bridge; I. Holland Tableting Science, Nottingham, UK), which were coupled with displacement transducers (linear potentiometer, 1,000×). Upper and lower punch data were recorded and transmitted on separate channels by individual amplifiers ("Boomerangs"). The amplifiers truncated the raw data from 16 to 12 bit after measuring to check IR transmission (data transmission rate—50 kBd, internal data buffer–1,024

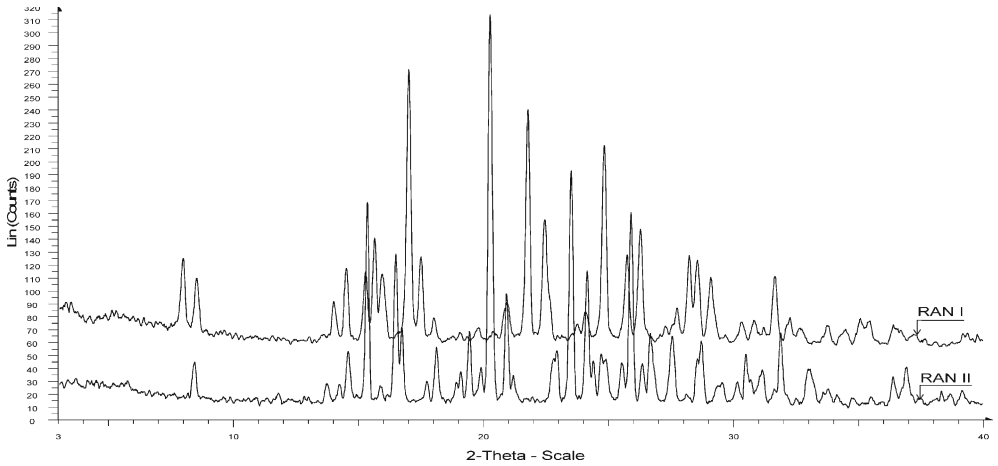

Fig. 1. PXRD overlay of forms I and II

measurement points). Analysis of compaction data was carried out by PPA analysis software (version 1.2, revision D, PuuMan Oy, Kuopio, Finland). Accuracy of force and displacement transducers was 1 and 0.02%, respectively. The suitability of the data acquisition system has been reported in the literature (8,9).

Calculation of Tablet Tensile Strength and Porosity

Breaking force of the tablets (n=3) was measured using a tablet hardness tester (tablet hardness tester, Erweka, USA). Tablet dimensions were measured using a digital caliper (Digimatic Mitutoyo Corporation, Japan). Tensile strength was calculated using Eq. 1 to eliminate the undesirable effect of variable tablet thickness on measured breaking force.

$$\sigma = {}^{2F}\!/_{\pi dt} \tag{1}$$

where σ is the tensile strength (in megapascal), F is the observed breaking force (in newton), d is the diameter (in millimeter), and t is the thickness of the compact (in millimeter).

The porosity, ε of the tablets (n=3) was calculated by the Eq. 2,

$$\varepsilon = 1 - {}^{\rho_c}\!/_{\rho_t} \tag{2}$$

Table I. Melting Point, Moisture Content, and True Density of RAN Polymorphs

Polymorph	Melting point (°C)	Moisture content (% w/w)[a]	True density (g/mL)[a]
Form I	135.05	0.12 (0.01)	1.374 (0.006)
Form II	138.50	0.11 (0.01)	1.342 (0.001)

[a] Standard deviations are reported in parentheses

where ρ_c is the density of the tablet calculated from the weight and volume of the resulting tablet. ρ_t is the true density of powder.

Statistical Analysis

Statistical significance for values of various compaction parameters were compared using a one-way ANOVA analysis (GraphPad Prism 6.0; GraphPad Software Inc., San Diego, CA) and the test was considered to be statistically significant if P<0.05.

RESULTS

Solid State Characterization of RAN Polymorphs

Figure 1 shows PXRD overlays for forms I and II. Both forms compared well with the patterns reported in literature (10). DSC trace of form I showed a single melting endotherm at 135.05°C, which was immediately followed by a decomposition exotherm. Form II showed similar behavior with a sharp melting endotherm at 138.5°C (Table I). Both values compared well with reported values (10). Both the forms of RAN showed similar moisture content (Table I). It is critical to maintain similar moisture content for both forms, as it affects compaction behavior. True density of both forms (Table I) was in close agreement to the earlier reports on true density (11,12). Figure 2 depicts particle morphology of ranitidine hydrochloride polymorphs. Form I particles were spherical agglomerates with smooth surface. Form II particles were also spherical agglomerates but relatively coarse surfaced as compared to form I.

Single Particle Fracture Strength

The nominal fracture strength (τ_{0s}) for each particle was calculated using Eq. 3.

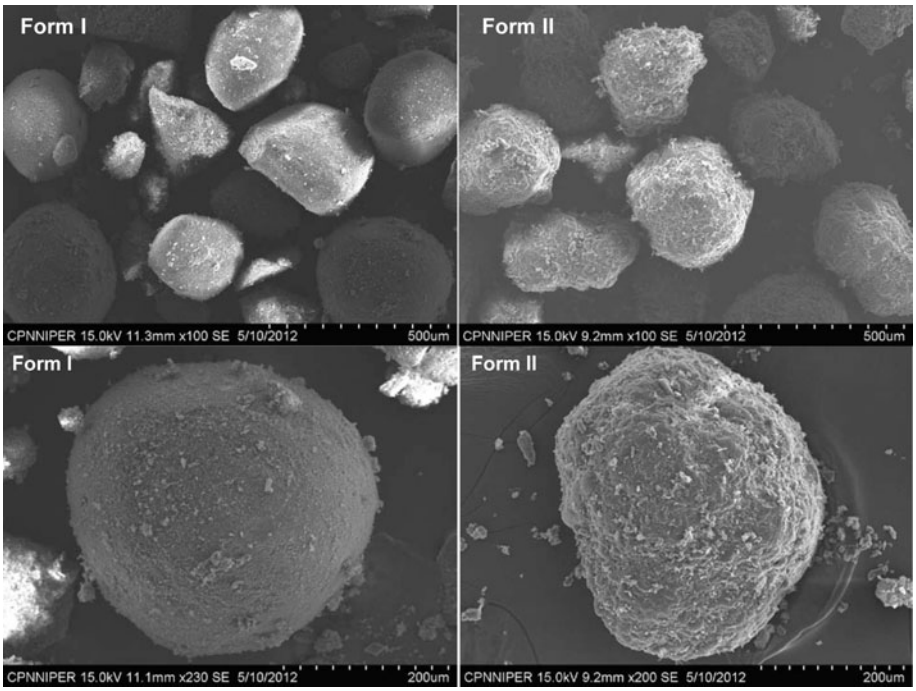

Fig. 2. Particle morphology of RAN polymorphs

$$\tau_{0s} = 4F_{max}/\pi d^2 \quad (3)$$

where F_{max} is the maximum observed fracture force (Fig. 3) and d is the median diameter of the particle undergoing test. In both the polymorphs, nominal single particle fracture strength was decreased with decrease in particle size (Table II). However, form I showed higher nominal fracture strength as compared to form II at a given particle size (Table II).

Powder Characterization for Compaction Studies

As shown in Table III, five particle sized fractions were selected for compaction studies based on their flow behavior and sample availability. All five powders showed acceptable flow property that allowed use of a fully instrumented rotary tablet press. Tapped density of the five powders follows the order; IIA > IIB > IIC > > IB > IA.

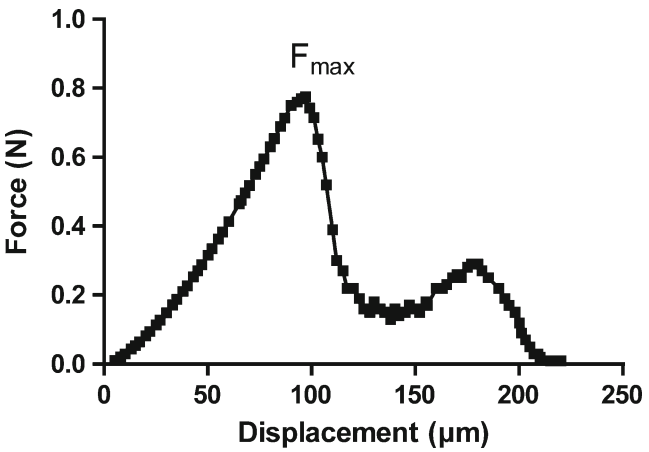

Fig. 3. Representative force–displacement profile of a single particle by microtensile testing

Out-of-die Compaction Behavior of RAN Polymorphs

Preliminary compaction studies were performed at very high compaction pressure (900 MPa) to rule out the possibility of polymorphic transformation. Both the forms were found stable, as no post-compaction solid form transformation was observed. Out-of-die compaction data of all five powders were obtained at various compaction pressures (0–400 MPa) using instrumented tableting press.

Tabletability

Tabletability is the capacity of a powdered material to be transformed into a tablet of specified strength under the effect of compaction pressure and is represented by a plot of tablet

Table II. Nominal Fracture Strength for Different Sized Particles of RAN Polymorphs

Polymorph	Particle size (μm)	Median particle size (μm)	Average nominal fracture strength (N/mm^2)[a]
Form I	650–800	700	3.40 (0.39)
	450–600	540	2.34 (0.12)
	300–400	340	1.71 (0.05)
Form II	650–800	720	1.79 (0.12)
	450–600	500	1.21 (0.08)
	300–400	360	1.05 (0.03)

[a] Standard deviations are reported in parentheses

Table III. Particle Size and Flow Behavior of RAN Polymorphs

Polymorph	Sample code	Particle size (μm)	D_{90}	D_{50}	Tapped density[a] (g/mL)	Carr's index	Flowability
Form I	IA	450–600	600	540	0.55 (0.006)	15.6	Good
	IB	300–400	400	360	0.57 (0.005)	27.1	Poor
Form II	IIA	450–600	600	500	0.90 (0.008)	11.3	Excellent
	IIB	300–400	400	340	0.87 (0.005)	13.5	Good
	IIC	150–180	180	160	0.85 (0.007)	19.8	Fair

[a] Standard deviations are reported in parentheses. IC size fraction showed very poor flow behavior and hence not characterized further

tensile strength against compaction pressure (5,13). Figure 4 shows tabletability plot for different sized fractions of RAN polymorphs. The tabletability of the given powders follows the order IB > IA > IIC > IIB > IIA. This indicates overall better tabletability of form I over form II. Tabletability of both the forms increases with decrease in particle size.

Tabletability was quantified in terms of a tensile strength achieved at the applied compaction pressure of 200 MPa. In case of IA, the compact formed at the compaction pressure of 200 MPa showed a tensile strength of 2.17 MPa. IB showed almost 135% increase in tensile strength over IA. On the other hand, compact of IIA exhibited a tensile strength of 0.9 MPa. The smallest sized fraction (IIC) of form II showed almost 175% increase in tensile strength over IIA at the same compaction pressure.

Compactibility

Compactibility is the ability of a material to produce tablets with sufficient strength under the effect of densification (13). It is represented by a plot showing tensile strength of the tablet against tablet porosity. Compactibility signifies the tensile strength of tablets normalized by tablet porosity. It may be used to quantify the interparticulate bonding strength of the materials. The ratio of tensile strength at a fixed porosity indicates relative interparticulate bonding strength. Form I showed greater compactibility as compared to form II at a given porosity (Fig. 5). However, different particle sized fractions of each polymorph showed overlapping compactibility profiles.

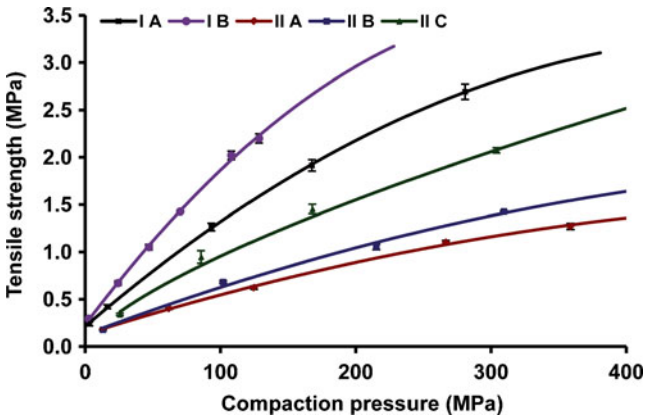

Fig. 4. Tabletability plot for different sized fractions of RAN polymorphs

Compressibility

The compressibility of a material is its ability to be reduced in volume as a result of an applied pressure (13). It is represented by a plot of tablet porosity against compaction pressure (5). The compressibility plot shows the ease with which a powder bed undergoes volume reduction under compaction pressure. The powder compressibility is a measure of interparticulate bonding area. For a given powder, tablet porosity decreases with increasing compaction pressure. This indicates that bonding area increases with increasing compaction pressure. As shown in Fig. 6, the compressibility of the five powders follows the order IIC > IIB > IIA > IB > IA. Increased in compressibility with decrease in particle size was observed in both the forms. However, form II showed greater compressibility over form I at a given particle sized fraction and compaction pressure.

In-die Compaction Behavior of RAN Polymorphs

Force–displacement profiles of all five powders were obtained at low, medium, and high compaction pressure of 111.5 (7.2), 224.9 (3.9), and 312.5 (7.9)MPa, respectively, and were mathematically transformed to fit Heckel and Kawakita equations. In case of IB powder fraction, a maximum compaction pressure of 220 MPa was applied. Beyond this pressure, extensive capping and lamination was observed due to the excessive strain hardening.

Heckel Analysis

The Heckel equation provides a method for transforming a parametric view of the force and displacement data, to a

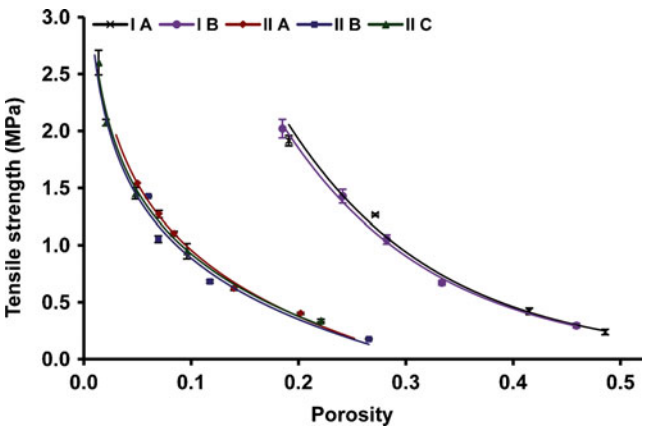

Fig. 5. Compactibility plot for forms I and II powders

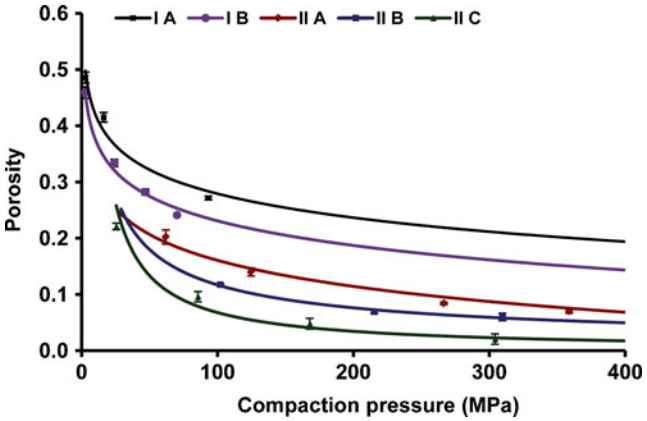

Fig. 6. Compressibility plot for different sized fractions of RAN polymorphs

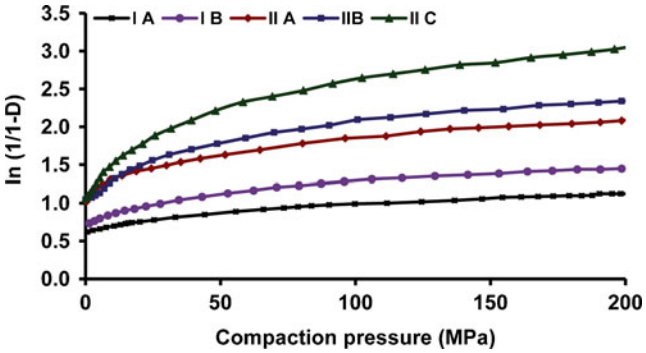

Fig. 7. In-die Heckel plots for different sized fractions of RAN polymorphs compacted at medium pressure

linear relationship for the materials undergoing compaction (14,15). It presents compaction behavior of the material in terms of its relative density under applied pressure (16). The basis for the equation for powder compression is that densification of the bulk powder under force follows first-order kinetics. The Heckel equation is expressed as Eq. 4.

$$\ln[1/1-D] = KP + A \tag{4}$$

where D is the relative density of the tablet (the ratio of tablet density to true density of powder) at applied pressure P, and K is the slope of straight line portion of the Heckel plot. Reciprocal transformation of the slope gives mean yield pressure, Py. Constant A gives densification of the powder due to initial particle rearrangement (Da) using Eq. 5.

$$\text{Da} = 1-e^{-A} \tag{5}$$

Linear regression was done on straight line portions of the Heckel plot between 25 and 100 MPa (R^2>0.99 in all cases), for studying the effect of particle size on densification (Fig. 7). Parameters obtained from Heckel analysis of the five sized fractions, each at different compaction pressure, are summarized in Table IV. Each value represents an average of six tablet measurements with their standard deviations in parentheses. Form I showed higher Py value than form II, at a given sized fraction and pressure. Py increased with increase in particle size and compaction pressure for both the polymorphs. At a given pressure, Py of five powders follows the order IIC < II B < IIA < IB < IA. Parameter Da, which describes densification due to initial particle rearrangement, increased with decrease in particle size and increased in compaction pressure. Form II showed higher Da as compared to form I at a given pressure and sized fraction.

Kawakita Analysis

Kawakita equation is based on the assumption that the particles subjected to compressive load are in equilibrium at all stages of compression, so that the product of pressure term and volume term is constant (17,18). Equation 6 described the Kawakita equation.

$$P/C = [P/a + 1/ab] \tag{6}$$

$$C = [(V_0-V)/V_0] \tag{7}$$

where P is the applied axial pressure and a is the value of initial porosity which corresponds to the total portion of reducible volume at maximum pressure. Mathematically, $1/b$ is simply the pressure needed to compress the powder to one half of the total volume reduction estimated as a term. b is proposed to be inversely related to the yield strength of particles (19). C is the degree of volume reduction (Eq. 7), V is volume of compact at pressure P, and V_0 is the initial apparent volume of powder.

Kawakita parameters a and $1/b$ were obtained from linear regression (R^2>0.99) of P/C *versus* P and results for different sized fractions are described in Table IV. Each value represents an average of six tablet measurements with their standard deviations in parentheses. Parameter $1/b$ for the five powders follows the order IIC < II B < IIA < IB < IA. Thus, form I showed higher values of $1/b$ when compared to form II at a given particle sized fraction and compaction pressure. The parameter $1/b$ that describes the yield strength increases with increase in particle size and compaction pressure. Form I showed higher values of parameter a over form II. Parameter a was found independent of compaction pressure.

DISCUSSION

Out-of-die Analysis

As discussed previously, compressibility and compactibility both contribute to tabletability and tensile strength is a product of the bonding area and the bonding strength. Decrease in porosity with increasing compaction pressure signifies increase in interparticulate bonding area while ratio of tensile strength at a fixed porosity indicates relative interparticulate bonding

Table IV. Heckel and Kawakita Parameters for Different Sized Powders of RAN Polymorphs

Compaction pressures (MPa)	Sample code	Heckel parameters		Kawakita parameters	
		Py (MPa)	Da	1/*b* (MPa)	*a*
111.5 (7.2)	IA	344.74 (4.6)	0.5085 (0.0004)	45.88 (2.3)	0.4079 (0.0001)
	IB	256.04 (3.2)	0.5413 (0.0011)	33.42 (1.3)	0.4049 (0.0021)
	IIA	149.11 (3.8)	0.7526 (0.0008)	18.71 (0.3)	0.3037 (0.0011)
	IIB	132.22 (1.2)	0.7637 (0.0002)	16.31 (0.5)	0.3142 (0.0035)
	IIC	75.22 (2.2)	0.7880 (0.0007)	10.22 (0.2)	0.3665 (0.0062)
224.9 (3.9)	IA	671.75 (6.7)	0.5677 (0.0013)	47.71 (1.8)	0.3937 (0.0009)
	IB	448.01 (1.3)	0.6786 (0.0010)	36.24 (1.6)	0.3856 (0.0044)
	IIA	199.16 (1.4)	0.7460 (0.0019)	23.12 (1.1)	0.2994 (0.0007)
	IIB	161.73 (3.8)	0.7712 (0.0017)	19.63 (0.9)	0.3082 (0.0008)
	IIC	91.22 (3.0)	0.8545 (0.0009)	14.42 (1.1)	0.3273 (0.0095)
312.5 (7.9)	IA	907.71 (4.2)	0.6547 (0.0021)	38.16 (0.4)	0.4111 (0.0022)
	IIA	369.76 (2.8)	0.8518 (0.0005)	24.38 (0.7)	0.3107 (0.0003)
	IIB	284.87 (7.2)	0.8788 (0.0059)	21.19 (0.2)	0.3282 (0.0031)
	IIC	173.13 (4.4)	0.8908 (0.0047)	18.60 (0.8)	0.3455 (0.0083)

Each value represents an average of six tablet measurements with their standard deviations in parentheses. Statistically significant difference was observed between values of each above-mentioned parameter for different particle sized fractions (P value<0.05). IC showed very poor flow behavior and hence not selected for compaction studies. In case of IB, data could not be obtained at higher compaction pressure (312.5 MPa) due to the excessive strain hardening

strength (1). Thus, tabletability signifies the tensile strength of the material under the effect of compaction pressure and can be used as a performance criterion for mechanical perfection (20).

In the present study, almost similar shape of the different sized fractions of the both forms enabled us to study the effect of particle size on compaction behavior of RAN (Fig. 2). Tabletability of both forms improved with decreasing particle size (Fig. 4). Varying particle size range from 450–600 μm (A) to 300–400 μm (B), in case of form I, showed 135% increase in tensile strength at the compaction pressure of 200 MPa. While in case of form II, decrease in particle size from 450–600 μm (A) to 150–180 μm (C), increased the tensile strength by 175%. Thus, particle size significantly improved the tabletability of the both polymorphs of RAN. Decrease in particle size offered larger surface area and greater contact points. Hence, smaller sized fractions of the both forms showed greater compressibility (Fig. 6) and hence tabletability.

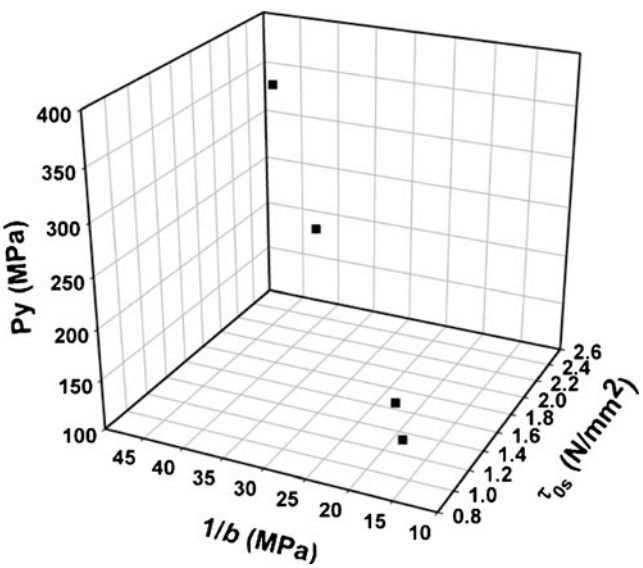

Fig. 8. Interrelationship between the in-die parameter by Heckel (Py), Kawakita (1/*b*), and the nominal fracture strength (τ_{0s}) derived from single particle fracture

Although, the smallest particle size of form II (IIC) improved tabletability significantly, it was still lesser than that of larger particle sized fraction of form I (IA). This can be explained further using compressibility and compactibility analysis. Figure 5 shows higher compactibility of form I over form II. In both forms, particle size did not influence compactibility. This is in accordance with our previous observation (5). Compressibility plot (Fig. 6) revealed greater compressibility of form II at a given compaction pressure and sized fraction. Decrease in particle size also improves the compressibility of both the forms. As discussed above, for a given form, compactibility remained same despite change in particle size. Hence, for a given polymorph, improved tabletability of smaller sized particles was attributed to their increased compressibility.

Bonding area–bonding strength concept (1) can be used to explain this further. For a given polymorph, increase in tensile strength of a smaller sized fraction was attributed to greater interparticulate bonding area. However, form II possesses poor bonding strength as compared to form I. Since, both bonding strength and bonding area contribute to tensile strength; form I, despite poor compressibility (lower bonding area) showed greater tensile strength by virtue of its higher bonding strength. Particle size governs the bonding area and does not contribute to bonding strength. Hence, for a given polymorph, different particle sized fractions showed similar compactibility. Lesser tensile strength of IIC than that of IA was also attributed to the reduced bonding strength of form II over form I. Therefore, we can conclude that tensile strength of RAN polymorphs was governed by bonding strength rather than bonding area.

In-die Analysis

Compaction comprises of two processes, namely compression and consolidation. Compression involves initial packing by particle rearrangement and densification while consolidation involves interparticulate bond formation by

particle deformation. In-die analysis allows us to study these two processes individually.

Particle Rearrangement

In-die analysis provides basic insights into initial packing of the particles during compression stage. Heckel (Da) and Kawakita (*a*) parameters were determined to study the initial packing behavior of RAN particles. Lower values of Da were obtained for form I particles at all the compaction pressures indicating their lower propensity towards particle rearrangement and densification. Propensity towards particle rearrangement increases with decreasing particle size and is evident by increasing value of Da (II A < II B < IIC or IA < IB). Higher relative density of the smaller sized fractions (Fig. 7) can be explained by higher particle rearrangement of the smaller particles at initial stage. Values of Da increases with increasing compaction pressure, as particles rearrangement increases with compaction pressure.

Kawakita parameter *a* describes the initial porosity at zero pressure which corresponds to the total portion of reducible volume at maximum pressure. Form I showed higher values of *a* at all compaction pressures indicating higher initial porosity as compared to form II. Initial porosities indicated by parameter *a* for the different particle sized fractions were found in accordance with tapped density data. Parameter *a* essentially follows reverse order (IA > IB > IIC > IIB > IIA) as that of tapped density because lower tapped density indicates higher porosity of the tablet bed.

Particle Deformation

The plot of measured compaction pressure as a function of relative density (Fig. 7) showed elastoplastic deformation of the two polymorphs. Form II showed better deformation behavior as compared to form I at a given compaction pressure and size faction. In both the forms, values of relative densities increased, with decreasing particle size, indicating a higher degree of densification for the smaller particles as compared to larger particles. Consequently, Py values were found to decrease with decreasing particle size at all the compaction pressures (Table IV). The values of 1/*b* which indicates a force required to reduce a volume to half of its original were higher for form I, at a given compaction pressure and size fraction (Table IV). Thus, greater force is required to reduce the volume to one half for form I. For a given polymorph, 1/*b* values decreases with decreasing particle size, again pointing towards higher deformation of smaller particles as compared to larger one. Results of Kawakita analysis are in agreement with Heckel analysis and a good correlation exists between 1/*b* parameter and Py (R^2>0.99) at all the compaction pressures. Moreover, both parameters showed pressure dependency. Lower values of Py and 1/*b* obtained for smaller particles correlated well with their compressibility. Higher compressibility leads to better deformation and lower yield strength. Higher plastic deformation offered greater bonding area to the smaller sized fractions.

As indicated by compressibility, Heckel and Kawakita analysis, form I resists densification under compaction pressure and yields at higher pressure. This can be explained by higher nominal fracture strength observed for form I particles in microtensile testing. This behavior can also be attributed to higher bonding strength of form I. As shown in Fig. 8, a good correlationship was obtained between the in-die measurement of yield strength by Heckel (Py), Kawakita (1/*b*), and the nominal fracture strength (τ_{0s}) derived from single particle fracture. This was in accordance with our previous finding (8). Particles with lower nominal fracture strength easily undergo deformation under the compaction pressure and yield at lower pressure. This was reflected in their lower Py and 1/*b* values.

In present work, we demonstrated that though particle size altered the compressibility, polymorph having higher true density still showed higher tensile strength by virtue of its greater compactibility. Compactibility is essentially independent of tableting speed (21) and descriptor based on compactibility can be used to predict tablet strength during formulation scale up and technology transfer.

CONCLUSION

Form I, despite poor compressibility and deformation behavior showed greater tabletability over form II by virtue of its higher compactibility. In case of both the polymorphs, tabletability improved with decreasing particle size. Larger particle size fraction of form I (IA) showed higher tabletability than that of the smallest particle size fraction of form II (IIC). This points towards contribution of compactibility rather than compressibility towards tabletability of RAN polymorphs. As reported previously, true density correlated well with compactibility or interparticulate bonding strength of the material and, hence, tensile strength prediction based on true density value may yield a better result. This may aids in selection of appropriate solid form and excipients for formulation development.

REFERENCES

1. Sun CC. Decoding powder tabletability: roles of particle adhesion and plasticity. J Adhes Sci Technol. 2011;25(4–5):483–99.
2. Sun CC. Materials science tetrahedron—a useful tool for pharmaceutical research and development. J Pharm Sci. 2008;98:1–17.
3. Sun C, Grant DJW. Influence of crystal structure on the tableting properties of sulfamerazine polymorphs. Pharm Res. 2001;18(3):274–80.
4. Upadhyay P, Khomane KS, Kumar L, Bansal AK. Relationship between crystal structure and mechanical properties of ranitidine hydrochloride polymorphs. Cryst Eng Comm. 2013;15(19):3959–64.
5. Khomane KS, More PK, Bansal AK. Counterintuitive compaction behavior of clopidogrel bisulfate polymorphs. J Pharm Sci. 2012;101(7):2408–16.
6. Khomane KS, More PK, Raghavendra G, Bansal AK. Molecular understanding of the compaction behaviour of indomethacin polymorphs. Mol Pharm. 2013;10(2):631–9.
7. Sun C, Grant DJW. Effects of initial particle size on the tableting properties of L-lysine monohydrochloride dihydrate powder. Int J Pharm. 2001;215(1):221–8.
8. Patel S, Kaushal AM, Bansal AK. Effect of particle size and compression force on compaction behavior and derived mathematical parameters of compressibility. Pharm Res. 2007;24(1):111–24.
9. Matz C, Bauer-Brandl A, Rigassi T, Schubert R, Becker D. On the accuracy of a new displacement instrumentation for rotary tablet presses. Drug Dev Ind Pharm. 1999;25(2):117–30.
10. Mirmehrabi M, Rohani S, Murthy KSK, Radatus B. Characterization of tautomeric forms of ranitidine hydrochloride: thermal analysis, solid-state NMR, X-ray. J Cryst Growth. 2004;260(3–4):517–26.

11. Ishida T, In Y, Inoue M. Structure of ranitidine hydrochloride. Acta Crystallogr C. 1990;46(10):1893–6.
12. Hempel A, Camerman N, Mastropaolo D, Camerman A. Ranitidine hydrochloride, a polymorphic crystal form. Acta Crystallogr C. 2000;56(8):1048–9.
13. Joiris E, Martino PD, Berneron C, Guyot-Hermann A-M, Guyot J-C. Compression behavior of orthorhombic paracetamol. Pharm Res. 1998;15(7):1122–30.
14. Heckel RW. Density–pressure relationships in powder compaction. Trans Metall Soc AIME. 1961;221(4):671–5.
15. Heckel RW. An analysis of powder compaction phenomena. Trans Metall Soc AIME. 1961;221:1001–8.
16. Ilkka J, Paronen P. Prediction of the compression behaviour of powder mixtures by the Heckel equation. Int J Pharm. 1993;94(1–3):181–7.
17. Kawakita K, Ludde KH. Some considerations on powder compression equations. Powder Technol. 1971;4(2):61–8.
18. Kawakita K, Hattori I, Kishigami M. Characteristic constants in Kawakita's powder compression equation. J Powder Bulk Solids Technol. 1977;1:3–8.
19. Nicklasson F, Alderborn G. Analysis of the compression mechanics of pharmaceutical agglomerates of different porosity and composition using the Adams and Kawakita equations. Pharm Res. 2000;17(8):949–54.
20. More PK, Khomane KS, Bansal AK. Flow and compaction behaviour of ultrafine coated ibuprofen. Int J Pharm. 2012;441(1–2):527–34.
21. Tye CK, Sun CC, Amidon GE. Evaluation of the effects of tableting speed on the relationships between compaction pressure, tablet tensile strength, and tablet solid fraction. J Pharm Sci. 2004;94(3):465–72.